Original Article

Effect of Annealing Time on Structural and Magnetic Properties of $Fe_{68}Pd_{32}$ Nanoparticles Synthesized by Sonoelectrodeposition

Nguyen Hoang Nam[1,2], Nguyen Tien Hoi[1], Truong Thanh Trung[1], Tran Thi Hong[1], Luu Manh Quynh[1], Nguyen Hoang Luong[1,2,*]

[1]VNU University of Science, Vietnam National University, Hanoi, 334 Nguyen Trai, Thanh Xuan, Hanoi, Vietnam
[2]Vietnam Japan University, Vietnam National University, Hanoi, Luu Huu Phuoc, Nam Tu Liem, Hanoi, Vietnam

Abstract: $Fe_{68}Pd_{32}$ nanoparticles were prepared by sonoelectrodeposition with subsequent annealing at 600 ºC for a series of times from 1 h to 6 h. The annealing transformed disordered face-centered cubic (fcc) phase in the as-prepared samples into a multi-phase material containing an ordered $L1_0$ FePd, fcc FePd and body-centered cubic (bcc) Fe phases. After annealing at 600°C for 6 h the hard magnetic phase $L1_0$-FePd and soft magnetic fcc-FePd phase coexist. The structural and magnetic properties of the samples were studied in dependence of annealing time. The decrease of coercivity with increasing annealing time from 1 h to 4 h is suggested to occur by formation of multi-$L1_0$ domain particles, while the increase of coercivity with increasing annealing time from 4 h to 6 h is proposed due to the multiphase nature of the nanoparticles samples.

Keywords: FePd, sonoelectrodeposition, magnetic nanoparticles, coercivity.

1. Introduction

FePd alloys with large magnetocrystalline anisotropy have been attracting considerable interest for their potential use in ultrahigh-density magnetic recording storage and high-performance permanent

___

magnets [1, 2]. FePd alloys containing about 30 at. % Pd are also considered attractive candidates for several applications because they show a ferromagnetic behavior at room temperature (see, for instance, [3] and references therein). As far as the Fe-rich FePd nanomaterials are concerned, much attention is paid on the thin films, while the data on nanoparticles are scarce. The as-prepared FePd nanoparticles are in the disordered face-centered cubic (fcc) phase. It is known that this disordered fcc phase in FePd nanoparticles is transformed into a multi-phase material containing an ordered $L1_0$ FePd phase by appropriate annealing. The existence of a multiphase in annealed samples is one of the important features of the $L1_0$ nanomaterials [4, 5]. It is of considerable interest to study the influence of the multiphase on structural and magnetic properties of the FePd nanoparticles. In this work, the effect of annealing time on structural and magnetic properties of Fe-rich FePd nanoparticles prepared by sonoelectrodeposition is investigated.

2. Experimental

The FePd nanoparticles were prepared by sonoelectrodeposition as described in [4]. The iron(II) acetate [$Fe(C_2H_3O_2)_2$], palladium(II) acetate [$Pd(C_2H_3O_2)_2$] and Na_2SO_4 were mixed under (Ar + 5%H_2) atmosphere in the electrolysis cell of 100 ml volume. The mixture was then sono-electrically deposited for 4 h by using ultrasound emitter (Sonics VCX 750) with power density of 100 W/cm^2, on/off current pulse of 500 ms/800 ms. The obtained FePd nanoparticles were washed, collected by using a centrifuge (Hettich Universal 320) at 8000 rpm for 30 min and then dried in air at 70°C for 30 min. The as-prepared FePd nanoparticles were annealed under (Ar + 5%H_2) atmosphere at 600°C for 1, 2, 4 and 6 h.

The structure of the as-prepared and annealed samples was studied by X-ray diffractometer (XRD) D5005, Bruker. The chemical composition of our sample was $Fe_{68}Pd_{32}$ as revealed from measurements of energy dispersive spectroscopy (EDS) included in scanning electron microscope (SEM) JSM-IT100, JEOL.

The average crystallite size, d, was calculated using Scherrer formula:

$$d = \frac{0.9\lambda}{B\cos\theta}$$

where λ is wavelength of the X-ray used (λ = 0.15406 nm), B - full half-maximum width (FHMW) in radians and θ - the Bragg angle of the considered diffraction peak [6].

Magnetic properties of the samples were studied using a vibrating sample magnetometer (VSM) at room temperature.

3. Results and Discussion

Figure 1 shows the XRD patterns of the as-prepared and annealed $Fe_{68}Pd_{32}$ nanoparticles for 1, 2, 4 and 6 h. Clear peaks are observed at 2θ from 35° to 55°. Typical peaks centered at 40.1° and 46.1° obtained from the XRD of the as-prepared sample show the X-ray diffraction from the (111) and (200) planes of face-centered cubic Pd (fcc-Pd) with a lattice constant of 3.902 ± 0.009 Å. This lattice constant is close to the lattice constant of 4N purity Pd (~3.890 Å) corresponding to the interstitial and substitutional occupation of iron atoms in the fcc-Pd lattice [4]. After 1-h annealing, the peaks centered at 40.1° and 46.1° disappear; and new peaks arise at 41.2°, 44.6°, 47.1°, 48.0° and 49.3°. The peak at 41.2° occurred in region I (from 39° to 42°) corresponds to the X-ray diffraction on (111) plane of the fcc γ-FePd and face-centered tetragonal (fct) $L1_0$ FePd phases [7]. In region II from 44.2° to

45.3°, the diffraction peak arose at 44.6° matches the diffraction peak of body-centered cubic Fe (bcc-Fe) at (111) plane and disappears as the annealing time increases from 1 h to 6 h. The contributions of the diffraction from (200) plane of fcc-FePd and (200), (002) planes of $L1_0$ FePd ranges from 46° to 50° (region III), respectively, are characterized by three peaks at 48.0°, 47.1° and 49.3° [7].
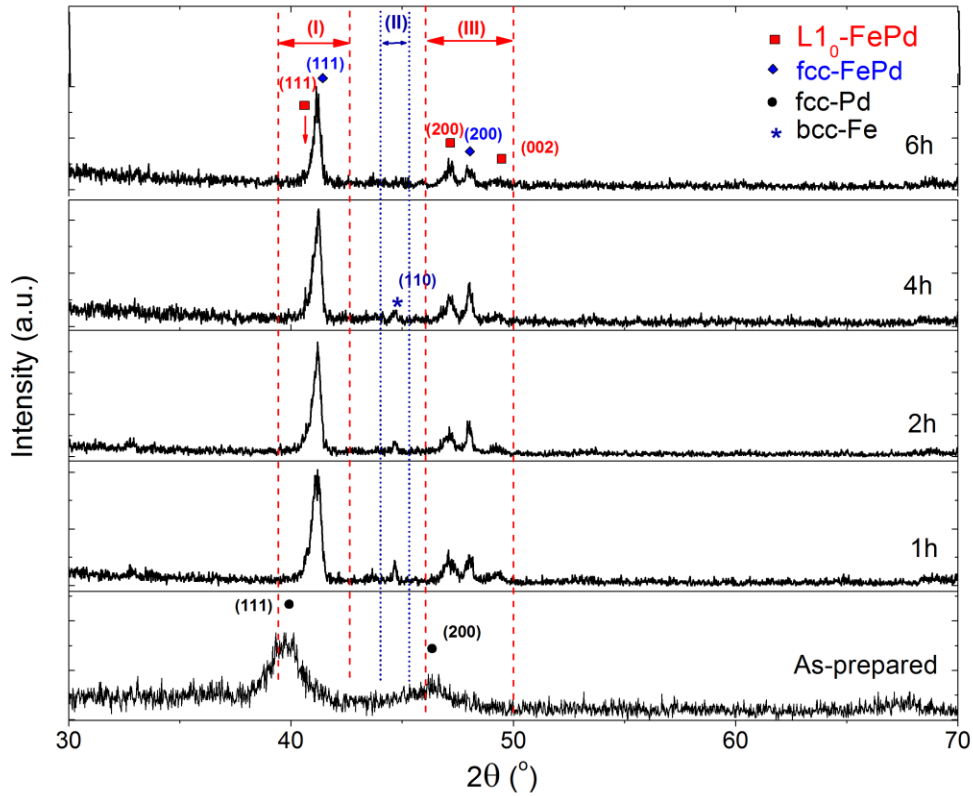
Figure 1. XRD patterns of the as-prepared and annealed $Fe_{68}Pd_{32}$ nanoparticles for 1 h, 2 h, 4 h and 6 h. I, II, and III are regions discussed in the text.

First we discuss the disappearance of the bcc-Fe during annealing. The XRD data observed at the region from 44.2° to 45.3° (region II) was fitted with a Gaussian curve. The fitting results are shown in Figure 2, from which the peak positions and the FHMWs are determined. The average crystallite sizes of the samples are estimated from the Scherrer formula. The average crystallite size of the bcc-Fe decreases from 60 nm to 30 nm as the annealing time increases from 1 h to 4 h. After annealing for 6 h, this peak is almost negligible following the dissolution of the bcc-Fe phase.

Secondly, it was achieved that the (111) peaks of the fcc γ-FePd and $L1_0$ FePd phases are overlapped each other around 41° (Figure 1) [4, 7]. The position of fcc γ-FePd (111) peak might occur at lower diffraction angle than that of $L1_0$ FePd (111) peak. Higher Fe composition in FePd alloy creates the decrease of the lattice constant of crystal, hence leads to the shift of the peaks to higher diffraction angles [8]. As consequence, the fcc γ-FePd (111) peak position can also locate at higher diffraction angle than the $L1_0$ FePd (111) peak position. In order to distinguish the positions of these two mentioned peaks, the data at the region I from 39° to 42° are fitted with a sum of 2 Gaussian functions by Gnuplot program in comparison with the fitting at the region III from 46° to 50° – corresponding to the (200), (002) of $L1_0$-FePd and (200) of fcc-FePd (Figure 3). The fitting results

show that the (111) peak of fcc-FePd locates at higher diffraction angle than that of L1$_o$-FePd, which is in a good agreement with our earlier study taking into account that the composition of the Fe in this study higher than in the samples studied in [4].
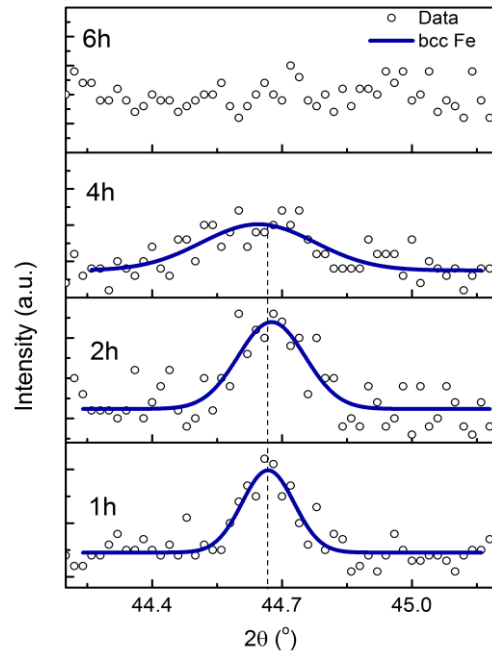
Figure 2. Fitting the XRD profile lines with Gaussian curves for the data selected from 44.2º to 45.3º (region II), which corresponds to the bcc-Fe crystal.
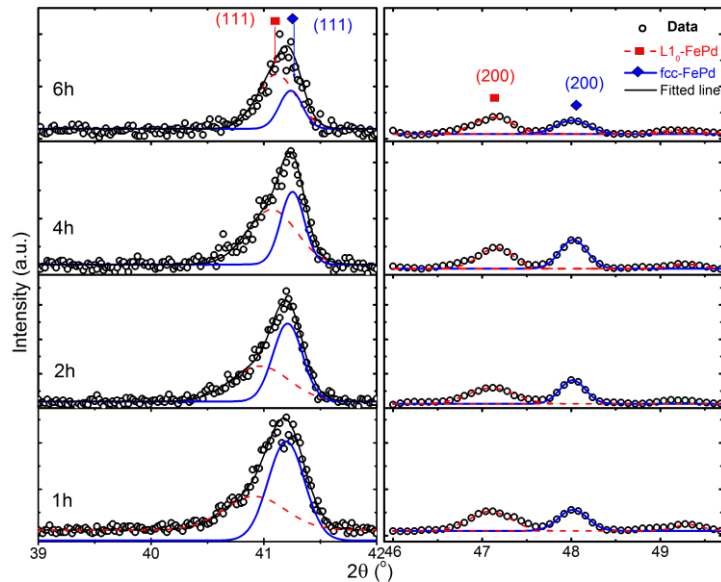
Figure 3. Fitting the XRD profile lines with Gaussian curves for the data selected from 39º to 42º (region I) and from 46º to 50º (region III), which corresponds to the L1$_0$- and fcc-FePd phases.

The lattice parameters and average crystallite sizes of the phases are estimated from the peak positions and FHWMs achieved from the Gaussian fitting and are shown in Figure 4. After annealing for 1 h, the average crystallite size of the fcc-FePd is larger than 23 nm, while the crystal size of the $L1_0$-FePd is smaller - about 13 nm, indicating that the fcc-FePd is more easily formed than $L1_0$-FePd. The same discussion was provided by Li and Hu [8], where the authors showed that the formation energy of fcc-FePd is lower than that of $L1_0$-FePd. With increasing annealing time from 1 h to 6 h, the average crystallite size of $L1_0$-FePd increases from 13 nm to 21 nm and that of fcc-FePd increases from 23 nm to 35 nm (see Figure 4). The size effect is experienced in the $L1_0$-FePd phase as "c" parameter of the unit cell of the tetragonal crystal decreases from 3.75 Å to 3.71 Å, while "a" parameter of the unit cell almost does not change. As the size of the particles being smaller, the lattice parameters increase by the interaction between the surface energy and elastic energy [9]. In $L1_0$-FePd crystal, c axis is the easy axis, hence it prefers to change rather than a axis. Besides, the fcc-FePd crystals are large enough that the size effect is not experienced followed by the unchanged lattice parameter.
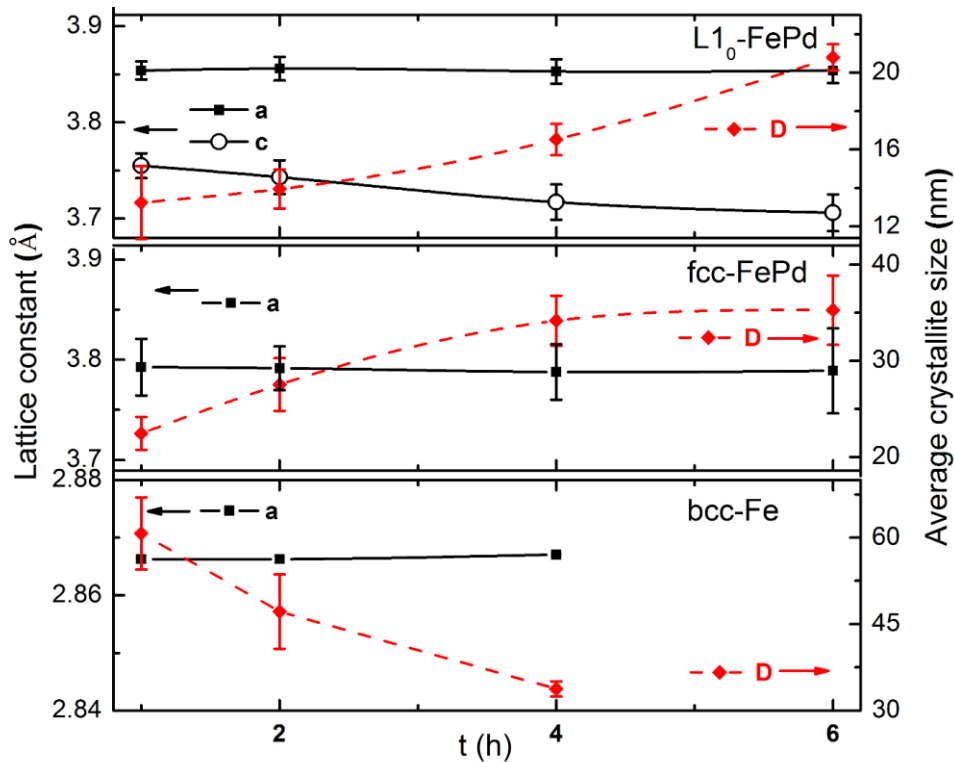
Figure 4. Lattice parameters and average crystallite sizes of the $L1_0$-FePd, fcc-FePd and bcc-Fe phases as a function of annealing time.

In agreement with our earlier research [4], right after the sonoelectrodeposition process, the FePd powder was created in disordered fcc-Pd. At 600 °C, the disordered fcc-Pd phase disappears; bcc-Fe intermediated phase is formed and grows to about 60 nm after annealing for 1 h. In parallel, stable $L1_0$-FePd and fcc-FePd phases arise. As the annealing time increases, the intermediate phase dissolves into the higher stability alloy, leading to the increase in size and amount of the $L1_0$-FePd and fcc-FePd phases.
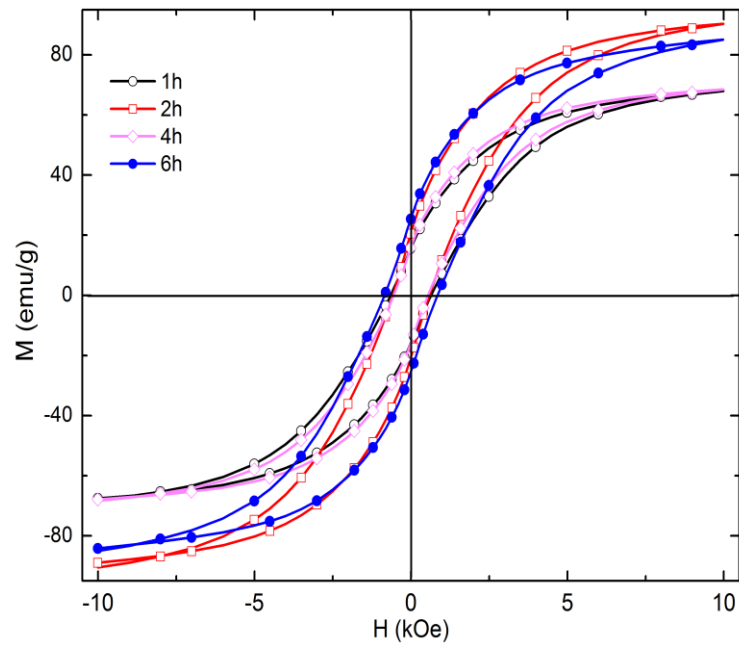
Figure 5. Magnetic hysteresis *M(H)* loops of $Fe_{68}Pd_{32}$ nanoparticles annealed for 1 h, 2 h, 4 h and 6 h.
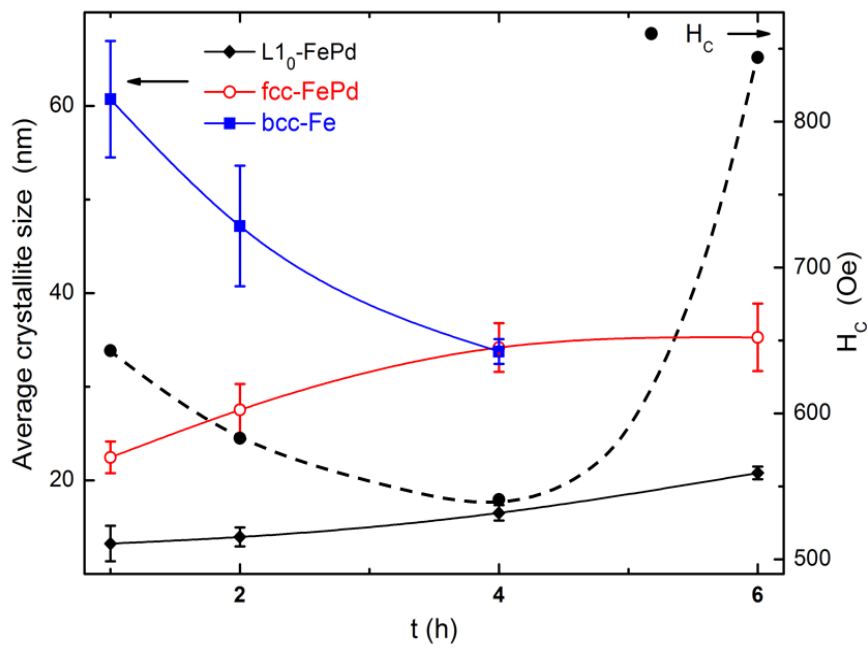
Figure 6. Average crystallite size and coercivity of $Fe_{68}Pd_{32}$ nanoparticles
as a function of annealing time.

Figure 5 presents magnetic hysteresis *M(H)* loops of the annealed $Fe_{68}Pd_{32}$ nanoparticles measured at room temperature. The loops show that the annealed samples exhibit ferromagnetic characteristics. The coercivity (H_C) values of 613, 583, 541 and 844 Oe were obtained for the sample annealed for 1, 2, 4 and 6 h, respectively. Thus H_C decreases with increasing annealing time from 1 h to 4 h, then abruptly increases with increasing annealing time from 4 h to 6 h. It is noted that Bahamida et al., [10] obtained the H_C value of 200 Oe for $Fe_{64}Pd_{36}$ thin films annealed at 600 °C for 1 h. Figure 6 displays the coercivity of $Fe_{68}Pd_{32}$ nanoparticles as a function of annealing time. Similar to the case of $Fe_{50}Pd_{50}$ nanoparticles [11], it can be speculated that the coercivity of our nanoparticles annealed for 2 h and 4 h is reduced probably because of formation of several multi-$L1_0$ domain particles by diffusion of Fe and Pd atoms upon annealing, leading to the reduction of magnetocrystalline anisotropy. With further increasing annealing time, the coercivity increases because $L1_0$ ordered region increases. XRD analysis shows that at annealing time of 6 h, the soft magnetic bcc-Fe phase is negligible, the hard magnetic $L1_0$-FePd phase and soft magnetic fcc-FePd phase coexist (see Figure 6), giving rise to exchange coupling between them. Under influence of this coupling magnetization reversal of the soft magnetic phase in applied field is difficult due to the presence of the hard magnetic phase, leading to the increase in coercivity.

4. Conclusion

$Fe_{68}Pd_{32}$ nanoparticles have been prepared by sonoelectrodeposition. The as-prepared nanoparticles are in the disordered fcc phase. Annealing at 600°C transforms the fcc phase into a multi-phase material containing an ordered $L1_0$ FePd, fcc FePd and bcc Fe phases. After annealing at 600°C for 6 h the hard magnetic phase $L1_0$-FePd and soft magnetic fcc-FePd phase coexist. The coercivity decreases with increasing annealing time from 1 h to 4 h, then abruptly increases with increasing annealing time from 4 h to 6 h. The decrease of coercivity is suggested to occur by formation of multi-$L1_0$ domain particles, while the increase of coercivity is proposed due to the multiphase (coexistence of $L1_0$-FePd and fcc-FePd phases) nature of the $Fe_{68}Pd_{32}$ nanoparticles.

Acknowledgments

References

[1] D. Weller, A. Moser, L. Folks, M. E. Best, W. Lee, M. F. Toney, M. Schwikert, J. U. Thiele, M. F. Doerner, High K_u Materials Approach to 100 Gbits/in^2, IEEE Trans. Magn. Vol. 36, No. 1, 2000, pp. 10-15.

[2] Z. Shao, S. Ren, Rare-earth-free Magnetically Hard Ferrous Materials, Nanoscale Adv., Vol. 2, No. 10, 2020, pp. 4341-4349.

[3] M. Salaheldeen, A. M. A. Dief, L. M. Goyeneche, S. O. Alzahrani, F. Alkhatib, P. A. Alonso, J. A. Blanco, Dependence of the Magnetization Process on the Thickness of $Fe_{70}Pd_{30}$ Nanostructured Thin Film, Materials, Vol. 13, No. 24, 2020, 5788 (12 pp).

[4] N. H. Luong, T. T. Trung, T. P. Loan, N. H. Nam, P. Jenei, J. Labar, J. Gubicza, Structure and Magnetic Properties of Nanocrystalline $Fe_{55}Pd_{45}$ Processed by Sonoelectrodeposition, J. Electron. Mater., Vol. 46, No. 6, 2017, pp. 3720-3725.

[5]   Y. Hong, I. de Moraes, G. G. Eslava, S. Grenier, E. Bellet-Amalric, A. Dias, M. Bonfim, L. Ranno, T. Devillers, N. M. Dempsey, A High Throughput Study of both Compositionally Graded and Homogeneous Fe-Pt thin films, J. Mater. Res. Technol., Vol. 18, 2022, pp. 1245-1255.

[6]   Cullity, B. D. Elements of X-Ray Diffraction, 2nd ed., Addison-Wesley Publishing Company, Inc., Reading, MA, 1978, pp. 102.

[7]   N. T. T. Van, T. T. Trung, N. H. Nam, N. D. Phu, N. H. Hai, N. H. Luong, Hard Magnetic Properties of FePd Nanoparticles, Eur. Phys. J. Appl. Phys., Vol. 64, No. 1, 2013, 10403 (4 pp).

[8]   C. M. Li, Y. F. Hu, Composition-dependent Properties and Phase Stability of Fe-Pd Ferromagnetic Shape Memory Alloys: A First-principles Study, J. Appl. Phys., Vol. 122, 2017, 245101 (7 pp).

[9]   W. H. Qi, M. P. Wang, Size and Shape Dependent Lattice Parameters of Metallic Nanoparticles, J. Nanopart. Res., Vol. 7, 2005, pp. 51-57.

[10] S. Bahamida, A. Fnidiki, M. Coisson, A. Laggoun, G. Barrera, F. Celegato, P. Tiberto, Mixed-exhange-coupled Soft α-($Fe_{80}Pd_{20}$) and Hard $L1_0$FePd Phases in $Fe_{64}Pd_{36}$ Thin Films Studied by First Order Reversal Curves, Mater. Sci. Eng. B, Vol. 26, 2017, pp. 47-56.

[11] N. H. Nam, N. T. B. Ngoc, T. T. Trung, T. T. Hong, P. T. Huong, N. H. Luong, CTAB-assisted Synthesis and Characterization of FePd Nanoparticles, VNU J. Sci: Math. Phys., Vol. 37, No. 3, 2021, pp. 1-8.